



# Blue intensity of Swiss stone pine as a high-frequency temperature proxy in the Alps

Riccardo Cerrato<sup>1</sup> · Maria Cristina Salvatore<sup>1,2</sup> · Marco Carrer<sup>3,4</sup> · Michele Brunetti<sup>4</sup> · Carlo Baroni<sup>1,2</sup>

Received: 4 July 2022 / Revised: 20 March 2023 / Accepted: 29 March 2023 / Published online: 18 April 2023  
© The Author(s) 2023

## Abstract

Tree rings are widely used for climatic reconstructions and for improving our understanding of ongoing climate change in high-altitude sensitive areas. X-ray maximum latewood density is a very powerful parameter to reconstruct past climatic variations, especially if compared to tree-ring width, but this method is neither inexpensive nor timesaving. However, blue intensity (BI) has resulted in an excellent maximum wood density surrogate that measures the intensity of reflected light from latewood in the blue spectra. This methodology is still considered a prototype parameter, and more data are needed for validation of the method. We present the first BI values coming from Swiss stone pine (*Pinus cembra* L.) collected on the southern margin of the Alps. Analyses were performed by testing different solvents and polishing techniques, as well as different CooRecorder pixel percentage settings. The results demonstrate that solvents and software parameters have little influence on the final chronologies. Dendroclimatic analyses demonstrate that Swiss stone pine BI can be a useful tool to extract at least the high-frequency variations in July–August temperatures with a correlation coefficient of up to 0.6 (over the 1800–2017 time period). The immunity of Swiss stone pine to insect defoliator outbreaks further enhances the reliability of the BI values of this species in reconstructing past high-frequency temperature variations in high-altitude sensitive areas.

**Keywords** *Pinus cembra* L. · Dendroclimatology · Dendrochronology · Blue intensity · Temperature sensitivity · Italian Alps

## Introduction

Tree rings are an important proxy widely used to study and understand climatic variation in the last millennium (Büntgen et al. 2006, 2011; Wilson et al. 2016; Anchukaitis et al. 2017). In fact, tree rings are used to obtain climatic information for periods of time and/or for remote areas in which instrumental data are not available (Cleaveland et al.

2003; Boninsegna et al. 2009; Yang et al. 2014; Wilson et al. 2016; Anchukaitis et al. 2017; Granato-Souza et al. 2019). High-altitude environments have been classified among the remote sites that are most threatened and sensitive to ongoing climate change. High-mountain environments are experiencing general glacier retreat, permafrost thawing and snow cover reduction that will induce changes in seasonal runoff and the total amount of water resources. This will have consequences not only on local natural, cultural and aesthetic aspects but also on lowland food productivity and water quality and availability (Immerzeel et al. 2020; Intergovernmental Panel on Climate Change (IPCC) 2022). In this respect, the identification of new proxies to help to understand past climate dynamics will improve our understanding of the consequences that climate change could have on such sensitive environments in the near future.

Various physical and chemical parameters of tree rings have been analysed, especially in recent decades (Björklund et al. 2019; Leavitt and Roden 2022). However, tree-ring width (TRW) is still the most popular parameter used for climatic reconstructions, although it has been demonstrated

---

Communicated by Ruediger Grote.

✉ Maria Cristina Salvatore  
mariacristina.salvatore@unipi.it

- <sup>1</sup> Dipartimento di Scienze della Terra, University of Pisa, Pisa, Italy
- <sup>2</sup> CNR-IGG, Consiglio Nazionale delle Ricerche–Istituto di Geoscienze e Georisorse, Pisa, Italy
- <sup>3</sup> Dipartimento Territorio e Sistemi Agro-Forestali, University of Padova, Padova, Italy
- <sup>4</sup> CNR-ISAC, Consiglio Nazionale delle Ricerche–Istituto di Scienze dell’Atmosfera e del Clima, Bologna, Italy

that maximum latewood density (MXD) can supply more accurate data in terms of target climate fidelity. A substantial improvement in palaeoclimatic reconstruction has been obtained by adding MXD chronologies (e.g., Briffa 2000; Büntgen et al. 2006; Schneider et al. 2015; Wilson et al. 2016) to the TRW proxy (Esper et al. 2018). In fact, MXD has not only been shown to share a higher variance with temperature but is also less affected by biological memory, thus representing an excellent temperature proxy (Esper et al. 2015, 2018; Ljungqvist et al. 2020). Despite this, MXD chronologies are still underrepresented compared to TRW, probably because of the fewer laboratories that are equipped to implement this methodology (Wilson et al. 2014, 2017b; Reid and Wilson 2020).

To overcome the costs of MXD analysis, a potential alternative has been identified in using the reflect blue light spectra (McCarroll et al. 2002), also known as blue intensity (BI). A recent study related BI values to cell-wall dimension rather than to lignin content (Björklund et al. 2021). The authors demonstrated that BI characteristics in terms of nonlinearity, temperature correlation strength, and autocorrelation are virtually identical to those expressed by MXD data (Ljungqvist et al. 2020). This evidence implies that BI could be considered a less expensive surrogate for the more expensive MXD. However, differences exist between BI and MXD datasets due to the intrinsic resolution of the methods (Björklund et al. 2019), which becomes even more evident when anatomical MXD is considered (Björklund et al. 2020; Seftigen et al. 2022). Despite BI has been tested on several conifers around the world, it is still considered a prototype parameter due to the difficulty of obtaining values that are unbiased by surface discolouration. BI studies have mainly focused on Scots Pine (*Pinus sylvestris* L.) in Fennoscandia (Campbell et al. 2007; Linderholm et al. 2010, 2015; Björklund et al. 2014, 2015, 2019, 2021; Fuentes et al. 2018; Seftigen et al. 2020) and Scotland (Wilson et al. 2012; Rydval et al. 2014, 2017a, b), on various *Picea* spp., *Pinus* spp. and *Tsuga* spp. in North America and Europe (Wilson et al. 2014, 2017a, 2019; Babst et al. 2016; Dolgova 2016; Buras et al. 2018; Nagavciuc et al. 2019; Heeter et al. 2019, 2020; Tsvetanov et al. 2020; Wang et al. 2020; Reid and Wilson 2020; Seftigen et al. 2022), and on various conifers species in Asia and Oceania (Buckley et al. 2018; Cao et al. 2020; Blake et al. 2020; Davi et al. 2021; Wilson et al. 2021; O'Connor et al. 2022). However, tests involving other tree species are required (Reid and Wilson 2020), especially in the European Alps, which is one of the core areas for dendroclimatic reconstructions in the Old World.

The two main species characterizing the treeline ecotone along the Alpine chain are European larch (*Larix decidua* Mill.) and Swiss stone pine (*Pinus cembra* L.). The TRW and MXD of European larch were largely used for millennial long temperature reconstructions (Büntgen et al. 2006, 2011;

Corona et al. 2010, 2011), although this species is the main host of the larch budmoth (*Zeiraphera diniana* Guénée), which alters the year-to-year tree-ring pattern with its regular outbreaks (Baltensweiler and Fischlin 1988; Esper et al. 2007; Büntgen et al. 2009, 2020; Cerrato et al. 2019a). Similarly, the TRWs of Swiss stone pine have often been used for climatic or glaciological reconstructions (Nicolussi 1995; Nicolussi et al. 1995; Büntgen et al. 2005; Corona et al. 2010; Leonelli et al. 2016), although the climate/growth response of this proxy proved to be unstable across the Alps (Oberhuber 2004; Carrer et al. 2007; Leonelli et al. 2011). Moreover, overly complacent ring width and latewood density have prevented the extensive use of Swiss stone pine MXD in investigations of climate/growth associations in the past (Schweingruber 1993). The species has thus far been overlooked in palaeoclimatic research. Nevertheless, recent studies performed in the southern sectors of the Alps, on the border of the natural distribution range of Swiss stone pine, have demonstrated that MXD and the anatomical traits of this species retain a higher (Carrer et al. 2018; Lopez-Saez et al. 2023) and more stable (Cerrato et al. 2019b) climate signal compared to TRW. Considering that Swiss stone pine rarely hosts defoliating insects (Nola et al. 2006) and considering the new evidence about its climate/growth association, it can be argued that this species could supply additional climatic information to those retrieved from European larch in high-elevation alpine environments. In this framework, the lack of knowledge about the possibility of using BI data as a climate proxy in Swiss stone pine represents an evident gap, also considering the paucity of density data from this taxon.

In this work, we present the potential use of BI to obtain climatic information from *Pinus cembra* L. in the Italian Alps. Tests on the preparation of the samples, utilizing the CooRecorder software settings for BI, in regard to the main driver of BI variation (i.e., lignin content or cell-wall dimension) and in regard to standardization methods were conducted to verify the main influencing factors. Finally, dendroclimatic analyses were performed to verify the sensitivity of BI as a temperature and precipitation proxy in the last two centuries (1800–2017) and its suitability for palaeoclimatic reconstruction purposes in high-altitude sensitive areas.

## Study area and climate

The study area is located in the Italian Alps in the western sectors of the Ortles-Cevedale Group. This region is characterized by a multitude of peaks exceeding 3000 m a.s.l. (e.g., Cevedale Mount–3761 m; P.ta dello Scudo–3466 m; P.ta Martello–3356 m; and Cima Lorchen–3347 m, Fig. 1), and it represents one of the highest glacierized areas in the Italian Alps (Salvatore et al. 2015). The sampled stand (10° 43' E, 46° 31' N), which belongs to a treeline ecotone, spans

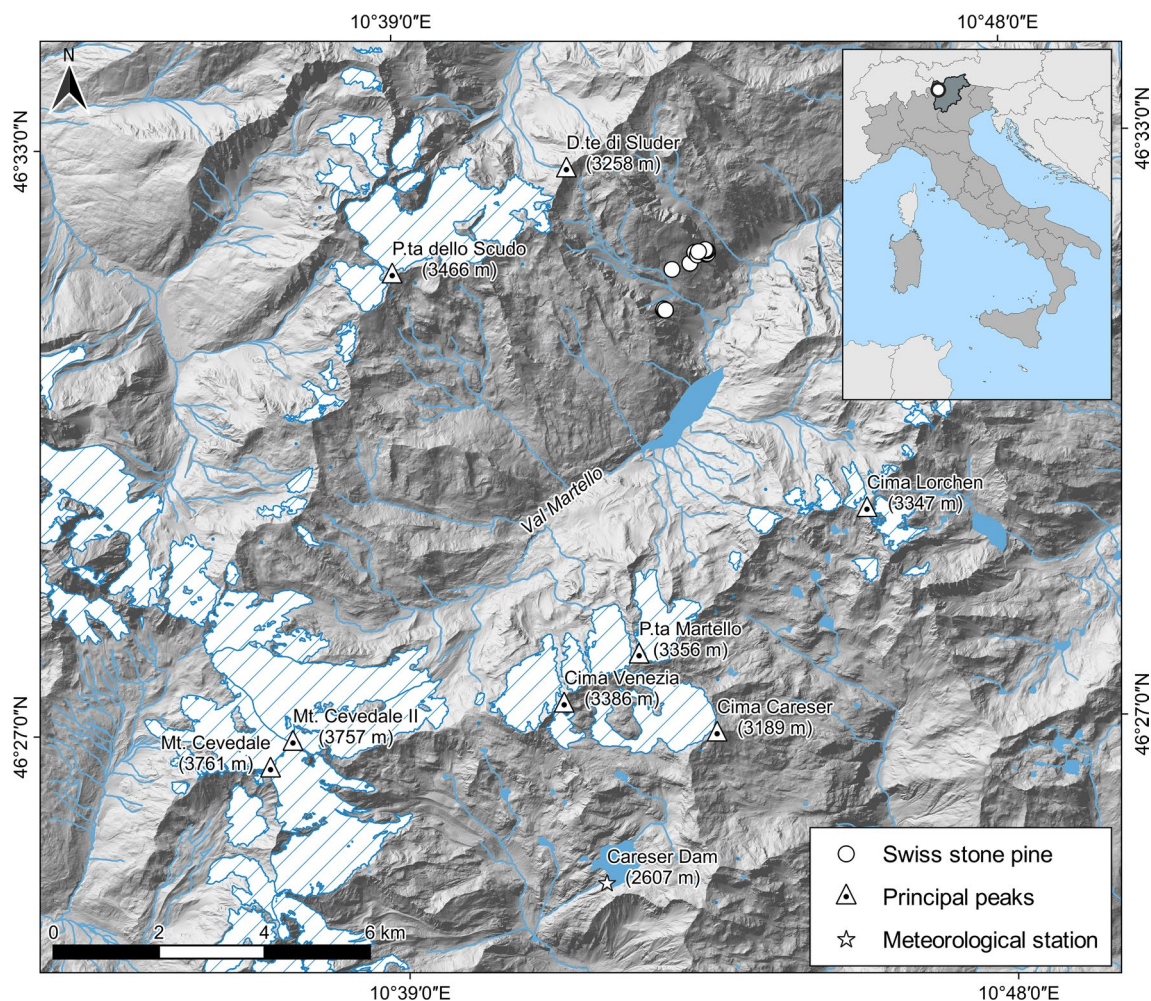


**Fig. 1** Location map of the study area. Glacial outlines refer to the 2006–2007 hydrological year (from Salvatore et al. 2015). Hydrography of Bolzano Province accessed through Web Features Service of the Open Data catalogue of the Provincia Autonoma di Bolzano—Agenzia per la Protezione Civile (last access: 2020-11-10). Hydrol-

ogy of Trento Province accessed through Web Features Service of the Portale Cartografico Trentino of the Provincia Autonoma di Trento (last access: 2020-11-10). White dots represent individual Swiss stone pine locations

between 2220 and 2330 m a.s.l. with a general south-eastern exposure. Swiss stone pine (*Pinus cembra* L.) individuals are scattered in an environment where ericaceous species are predominant [*Rhododendron ferrugineum* L., *Vaccinium* spp. (Andreis et al. 2005; Gentili et al. 2013, 2020)], but dominant trees are also present in association with European larch (*Larix decidua* Mill.) at the timberline belt at lower altitudes. Soils are commonly influenced by bedrock and superimposed vegetation and can be classified as immature and shallow podzols, histosols or umbrisols (IUSS Working Group 2007; Galvan et al. 2008).

The area located just south of the so-called inner dry Alpine zone (Isotta et al. 2014) features a latitudinal precipitation pattern, with increased precipitation from northern sectors towards the southernmost sector. The mean annual amount of precipitation is 928.4 mm, with the minimum in

winter and the maximum in late spring–summer (Carturan et al. 2012; Crespi et al. 2018). Winter (December–February, DJF) is the driest season (140.8 mm), while summer (June–August, JJA) is the wettest (288.1 mm). The annual mean temperature recorded from 1961 to 1990 at the Careser meteorological station (ca. 12 km southward at 2607 m a.s.l.) was  $-1.2$  °C, with February being the coldest month ( $-8.3$  °C) and July being the warmest ( $+6.9$  °C).

## Materials and methods

### Sampling and sample preparation

A total of 15 dominant and isolated individuals were sampled, giving particular attention to avoiding trees that clearly

showed physical damage. A 12-mm core was extracted from each selected tree at breast height by using an increment borer. Each sample was slowly air-dried and then sanded with progressively finer sandpapers up to P1200 until the ring boundaries were perfectly discernible. Tree-ring widths (TRW) were then measured with a precision of 0.01 mm by means of a LINTAB™ mod. 3 device connected to TSAP-Win Scientific 4.69 h software (RINNTECH®, Heidelberg, Germany). Visual cross-dating of the series was performed to identify missing rings, false rings, or measurement errors, and each dated series was then statistically verified using COFECHA software (Holmes 1983).

### Blue intensity data

To obtain a dust-free surface, cores were sectioned into segments of four to five cm and then trimmed with a semi-automated rotary microtome (Leica Camera AG, Wetzlar, Germany) using a stainless-steel microtome blade Model N35 (Feather, Osaka, Japan). The trimmed sections were then scanned at 3200 dpi using a flat-bed scanner Epson Perfection V850 Pro (Seiko Epson Corporation, Suwa, Japan) with SilverFast Archive Suite 8 software (LaserSoft Imaging AG, Kiel, Germany). Scanner acquisition colours were standardized using an IT8.7/2 colour card. BI values were then measured using Coorecorder 9.5 software (Cybis 2020—<http://www.cybis.se/forfun/dendro/index.htm>) using the TRW series as a reference due to the occurrence of very narrow rings.

The scientific literature has reported several solutions for calculating the BI value on the basis of species, site and scientific purpose (Rydval et al. 2014; Dannenberg and Wise 2016; Kaczka et al. 2018; Schwab et al. 2018; Buckley et al. 2018; Tsvetanov et al. 2020). In this study, minimum latewood BI values (LWBI) were measured considering a frame width and depth of 100 and 50 pixel, respectively (equal to 0.79 and 0.40 mm), whereas the maximum earlywood BI values (EWBI) were measured with a frame width and depth of 100 (0.79 mm) and 200 (1.59 mm) pixels, respectively. The location of the frame was set at 5 (0.04 mm) and –2 pixels (0.02 mm) for LWBI and EWBI, respectively. For both values, we considered the mean of the first to fourth quartiles of the darkest (lightest when considering the EWBI) pixels contained in the frame equal to 25%, 50%, 75% and 100% of the pixels, respectively (Fig. S1 in the Supplementary Material). Finally, BI values were inverted following a standard procedure (Rydval et al. 2014; Wilson et al. 2014). The differences between the EWBI and LWBI datasets were calculated by composing 16 different so-called Delta BI (DBI) datasets (Björklund et al. 2014, 2015).

Extractives (e.g., resin) are another well-known issue in BI studies, and even in this case, there are several solutions that depend on species, site, and purpose (Sheppard and

Wiedenhoef 2007; Rydval et al. 2014; Dolgova 2016; Wilson et al. 2017a; Arbella et al. 2018; Fuentes et al. 2018). In this study, the 15 individuals were divided into two groups of eight and seven individuals. The individuals belonging to the first group (G1, hereafter) that were trimmed and scanned a first time, were washed in a Soxhlet apparatus with ethanol at 96% for 72 h, and then the cores were slowly air-dried for 24 h in a vacuum hood before scanning a second time. Afterwards, the same individuals were washed in acetone at 99% for 72 h, air-dried for 24 h and then scanned a third time. Last, the samples were polished with sandpaper at P1200 and scanned for a fourth time (Fig. S2 in the Supplementary Material). The seven samples belonging to the second group (G2, hereafter) were processed equally to G1 but with the inverted order of solvents: the first wash was with acetone at 99%, whereas the second was with ethanol at 96%. To summarize the data, the BI values obtained from trimmed samples (i.e., dust-free ducts with extractives) were called “raw”; those obtained from sample washing one time (dust-free ducts), independently from the solvent used, were called “one\_wash”; those obtained from sample washing two times (dust-free ducts), independent of the order of the solvents, were called “two\_wash”; and those obtained from polished samples (dust-filled ducts) were called “polished”.

### Statistical analysis

The heartwood and sapwood portions of the raw and one\_wash series were analysed separately to verify the influence of the solvent used. As in the first phase, all individuals were analysed separately. The residual series between heartwood raw and one\_wash were tested for normality by means of a Shapiro test. A paired Wilcoxon (nonparametric) or T test (parametric) was subsequently used to test if the difference between the means of the raw and one\_wash series was significant at the 0.05 level. Parametric or nonparametric tests were preferred based on the normal distribution of the residuals. As a second phase, the mean heartwood BI value of the raw and one\_wash individual series was calculated and grouped by treatment (i.e., G1 and G2), and then the same tests as in phase one were performed on the groups and between groups. The same procedure was also applied to the sapwood series.

The expressed population signal (EPS) was calculated to estimate the influence of the treatments on the samples and the representativeness of the sampling compared to an infinite hypothetical population (Wigley et al. 1984). This parameter was calculated on the raw, single-washed, double-washed, and polished BI datasets without considering the order of the solvent treatments. To test which factor between cell dimension or wood lignin content was driving the BI, the EPS, mean correlation between individuals ( $r_b$ ) and correlation with climate of the two\_wash and polished series

were compared (further information can be found in the chapter “Blue intensity data/climate analysis”).

## Standardization

Several methods have been used recently to detrend the BI series of other conifer species with a prevalence of splines or age-adaptive spline methods with different initial stiffnesses coupled or not with a signal-free approach (Dolgova 2016; Wilson et al. 2017a; Buras et al. 2018; Nagavciuc et al. 2019; Heeter et al. 2019; Seftigen et al. 2020; Tsvetanov et al. 2020; Wang et al. 2020; Björklund et al. 2020; Reid and Wilson 2020). Other popular methods include linear regression (Campbell et al. 2011; Wilson et al. 2014, 2019; Brookhouse and Graham 2016; Rydval et al. 2017a, b) or regional curve standardization (Björklund et al. 2014, 2015; Fuentes et al. 2018). For this study, we opted to utilize spline detrending since the data did not show any negative exponential trend. Specifically, cubic splines with 50% variance cut-offs at 30, 100 and 200 years were also applied to the BI series in conjunction with a signal-free approach (as described in Melvin and Briffa 2008). Moreover, horizontal lines through mean and age-adaptive smoothing splines (described as Fortran 90 script in Melvin et al. 2007) with initial stiffnesses of 30, 100 and 200 years were applied to the BI series. Detrended series were calculated as ratios, and chronologies were obtained as biweight robust means (Fritts 1976; Schweingruber 1988). All processing was performed in the R statistical environment (Bunn 2008; R Core Team 2022).

## Climate dataset

To explore the sensitivity of the BI series to climatic variability, climatic information specific to the sampling site was reconstructed for the past two centuries by means of anomaly methods (Mitchell and Jones 2005) exploiting the large amount of instrumental data available for the area, starting from the late eighteenth century. The anomaly method is the most common method used to interpolate station series onto a specific point, preventing their different data availabilities from biasing the results. It consists in converting the temporal series into anomalies with respect to the same common reference period before interpolating them onto a specific point. Finally, the mean climate representative of the point itself is added to the interpolated series to convert its anomalies back into absolute values. Specifically, as described in Brunetti et al. (2012), the technique is based on the independent reconstruction of monthly climatologies (i.e., the mean climate values estimated over a specific reference period) and on their relative deviations (i.e., anomalies with respect to the same baseline period). Climatologies are characterized by strong spatial gradients that can be captured by many weather

stations (even if only available for a short period), together with an interpolation technique exploiting the dependence of climatic variables on orography. Anomalies linked to climate change and variability are characterized by higher spatial coherence. A limited number of stations with satisfactory temporal coverage are sufficient to capture spatial patterns through simpler interpolation methods, but data homogenization is mandatory. The data must be corrected for errors deriving from the history of the stations (changes of station and instrument location, instrument replacements, etc.), which masks the actual climate signal. Monthly temporal series were obtained by superimposition of the reconstructed climatologies and anomalies. In this work, the temperature (i.e., monthly mean values of maximum, minimum and mean temperature) and precipitation information were reconstructed from 1800 to 2017 for the analysis with the tree-ring series (Fig. S3 in the Supplementary Material for data availability of the dataset used to reconstruct the climatic information). Climate data were standardized by means of splines with a 50% frequency cut-off at 30, 100, and 200 years to minimize the bias in correlation with the BI datasets resulting from unfiltered trends (Cerrato et al. 2018, 2019b; Seftigen et al. 2020), and correlation values were calculated in the R statistical environment using the treeclim package (Zang and Biondi 2015).

## Blue intensity data/climatic analysis

The Pearson’s correlation values between BI chronologies and climate data were calculated for a period spanning from 1800 to 2017 and from May of the year before tree growth to the current October and for the means of the current July–August (JA), June–August (JJA) and May–September (MJJAS) periods, since previous studies have highlighted a positive correlation with these aggregated periods for the study area (Cerrato et al. 2019b). A correlation analysis was also performed by using a moving window of 50 years between 1800 and 2017 to test the time stability of the climatic signal.

## Results

### Tree-ring width chronology

With the 15 individuals, we built a site chronology spanning from 1707 to 2018 (312 years) with an average series length of 256 years. The mean series intercorrelation was 0.36 with an EPS of 0.89 (Table 1), and the mean series correlation with the biweighted mean chronology was equal to 0.54.

**Table 1** Number of samples, mean expressed population signal (EPS), and mean correlation between individual ( $r_{bt}$ ) values of different tree-ring parameters and treatments considered

	n. trees	Mean $r_{bt}$ *			Mean EPS*		
TRW	15	0.36			0.89		
BI		EWBI	LWBI	DBI	EWBI	LWBI	DBI
Raw	15	0.07	0.11	0.02	0.29	0.13	0.24
ethanol	8	0.09	0.17	0.02	0.22	0.45	0.13
acetone	7	0.07	0.06	0.03	0.13	-0.05	0.10
one_wash	15	0.07	0.11	0.02	0.38	0.47	0.21
ethanol~acetone	8	0.11	0.17	0.02	0.28	0.41	0.07
acetone~ethanol	7	0.04	0.01	-0.00	0.02	-0.39	-0.07
two_wash	15	0.08	0.09	0.02	0.39	0.37	0.20
ethanol~cetone polished	8	0.12	0.26	0.25	0.35	0.67	0.72
acetone~ethanol polished	7	0.00	0.09	0.21	-0.03	0.40	0.62
polished	15	0.04	0.15	0.23	0.33	0.69	0.81

\*Values are relative to the portion of chronology with an SSS value greater than 0.85 (Buras 2017)

## Blue intensity

The different washing steps and quartiles allowed us to obtain an assemblage of 480 BI datasets for performing several analyses. Regarding the quartiles, increasing the percentage of the considered pixels, the BI value returned for the latewood increased, whereas that returned for the earlywood decreased, as expected. However, during the calculation of the DBI, the means and standard deviations of the BI values were negatively correlated with the considered quartiles of both latewood and earlywood: the higher the considered percentage was, the lower the BI mean and standard deviation returned, indicating (i) a higher influence of the EWBI on the final value and (ii) a suppression of the extreme values that could occur when a limited number of pixels was considered.

Considering the effect of the solvents used, both affected series lowered the EWBI and LWBI values of one\_wash compared to raw, with the exception of the sapwood LWBI, where the BI values were equal to or higher than raw (Fig. S4 in the Supplementary Material). Considering the heartwood individual series, the differences in G2 were always significant, whereas in 9% of the cases in G1 (involving a series of 4 individuals), the difference was not statistically significant at the 0.05 level. Regarding sapwood, in 6% of the cases of both G1 and G2 (involving a series of 4 individuals, each), the difference between the raw and one\_wash series results was not statistically significant.

Consistent results were obtained by G1 and G2 analyses (i.e., considering the series of the mean values of the individual series) with lower EWBI and LWBI values shown by one\_wash compared to raw with the exception of the sapwood G1 EWBI and G2 LWBI, whose one\_wash mean values were not significantly different from those of the raw and sapwood G1 LWBI, which instead increased (Fig. 2). The difference between the mean heartwood BI raw and



**Fig. 2** Boxplot of raw and one\_wash BI values divided by solvent group and heartwood/sapwood portion and EWBI, LWBI, and DBI. Asterisks identify differences not significant at the 0.05 level

one\_wash values was always statistically significant. On average, the difference between the raw and one\_wash BI values was greater in G2 than in G1, but the difference in the mean difference between G1 and G2 was not significant, with the exception of the heartwood EWBI, which was significant at the 0.01 level. Regarding the DBI, the effect of the solvent was opposite to that observed on EWBI and LWBI: one\_wash DBI values were greater than raw and the difference of the means was statistically significant for both solvents used. Moreover, the difference between G1 and G2 was also statistically significant at the 0.001 level, with G2 returning higher DBI values (Fig. 2).

Considering the not detrended chronologies, the most important process that deeply affected BI values was polishing. In fact, the EWBI and LWBI of the raw, one\_wash and two\_wash datasets showed similar values and trends (Fig. 3), even if a slight separation between the raw sample and the washed sample was particularly evident in the less recent portion of the chronologies of G1 (before 1850 CE). The polished datasets had lower BI values (i.e., lighter colours in the visible, and thus blue, spectra) and a flatter trend compared to the raw and washed datasets. All datasets showed a decrease in BI values (lighter colour) starting from 1930 to 1950 CE, and this trend was more evident in unpolished datasets (Fig. 3). The DBI datasets, instead, showed similar and quite flat long-term trends considering the washed and polished chronologies, whereas the raw DBI dataset had a general decreasing tendency from the second half of the nineteenth century (Fig. 3).

Regarding the representativeness of the obtained chronologies of a hypothetical infinite population, the raw, one\_wash and two\_wash BI chronologies generally featured low and unstable EPS values. With the obtained EPS values, these chronologies could hardly be considered representative of the population. However, the raw DBI chronologies displayed slightly higher values than those shown by the DBI of one\_wash and two\_wash with a period of high diversity during the first half of the twentieth century (Fig. 4). Better results were supplied by the polished BI chronologies that generally showed high and stable EPS and  $r_{bt}$  values, closer to the commonly used threshold of 0.85, even with a relatively small sample depth (Fig. 4, Table 1).

## Detrending

Different standardization methods applied to the dataset returned very similar results, especially considering the polished series. Considering the raw, one\_wash, and two\_wash EWBI and LWBI series, more variability among the different standardization approaches seemed to exist, but the differences were flattened when the DBI was calculated. In these last cases, the portion of the DBI chronologies that preserved an appreciable difference related to the different standardization approaches was represented by the first hundred years; afterwards, all chronologies converged to the same values (Fig. S5 in the Supplementary Material). The only standardization method that returned appreciable differences, at least regarding the EWBI and LWBI, was the division by the mean from each series. However, even in this case, these differences were flattened when the DBI was calculated.

## Climate associations

The correlation values between BI parameters, climate datasets, sample treatments and detrending methods were consistent. Associations with precipitation always returned nonsignificant results, while significant values were only obtained when considering the correlation between temperatures (mean maximum, mean, and mean minimum) and polished LWBI and DBI chronologies (Fig. 5). BI chronologies built with raw samples treated with one or two solvent(s) and the chronologies built with EWBI polished samples only showed no, or a barely significant, correlation with temperature.

Regarding the standardization methods, the application of the signal-free procedure slightly decrease the correlation values that were always lower than those obtained by applying a simple cubic smoothing spline. Spline stiffness also seems to have had a greater influence on the LWBI than on the DBI chronologies with a negative relationship: the stiffer the spline was, the lower the correlation values. The same relationship was observed in the DBI and LWBI chronologies obtained by applying the age-dependent spline with different initial stiffnesses.

Considering the correlation with the monthly temperature, the highest values were obtained for August and July (Table 2), while at the seasonal level, the highest value was obtained with JA mean maximum temperature ( $0.60 \pm 0.006$ ) (Fig. 5, Table 2).

Moving correlations presented results that were consistent with static correlation. Considering the mean correlation results obtained from the analysis of all LWBI and DBI chronologies with mean maximum temperature data, the highest and most stable correlation values were obtained between JA aggregated mean maximum temperature and both LWBI and DBI (Fig. 6). The correlation value was more stable with the DBI than with the LWBI, showing a decrease during the 1880s–1920s with few nonsignificant years. Instead, the DBI temperature correlation showed a smaller decrease in correlation values in the 1940s–1970s but maintained its significance level always above 95%. Moreover, the standard deviations of the correlation values obtained from the DBI chronologies were much smaller than those obtained from the LWBI chronologies (Fig. 6).

## Discussion

We tested whether the BI parameter could provide relevant information for dendroclimatic purposes in Swiss stone pine. During dendroclimatological investigations in the Alps, this species has usually been overlooked, whereas other conifer species, namely, European larch and Norway spruce (*Picea abies* (L.) H. Karst.), have almost always been favoured.

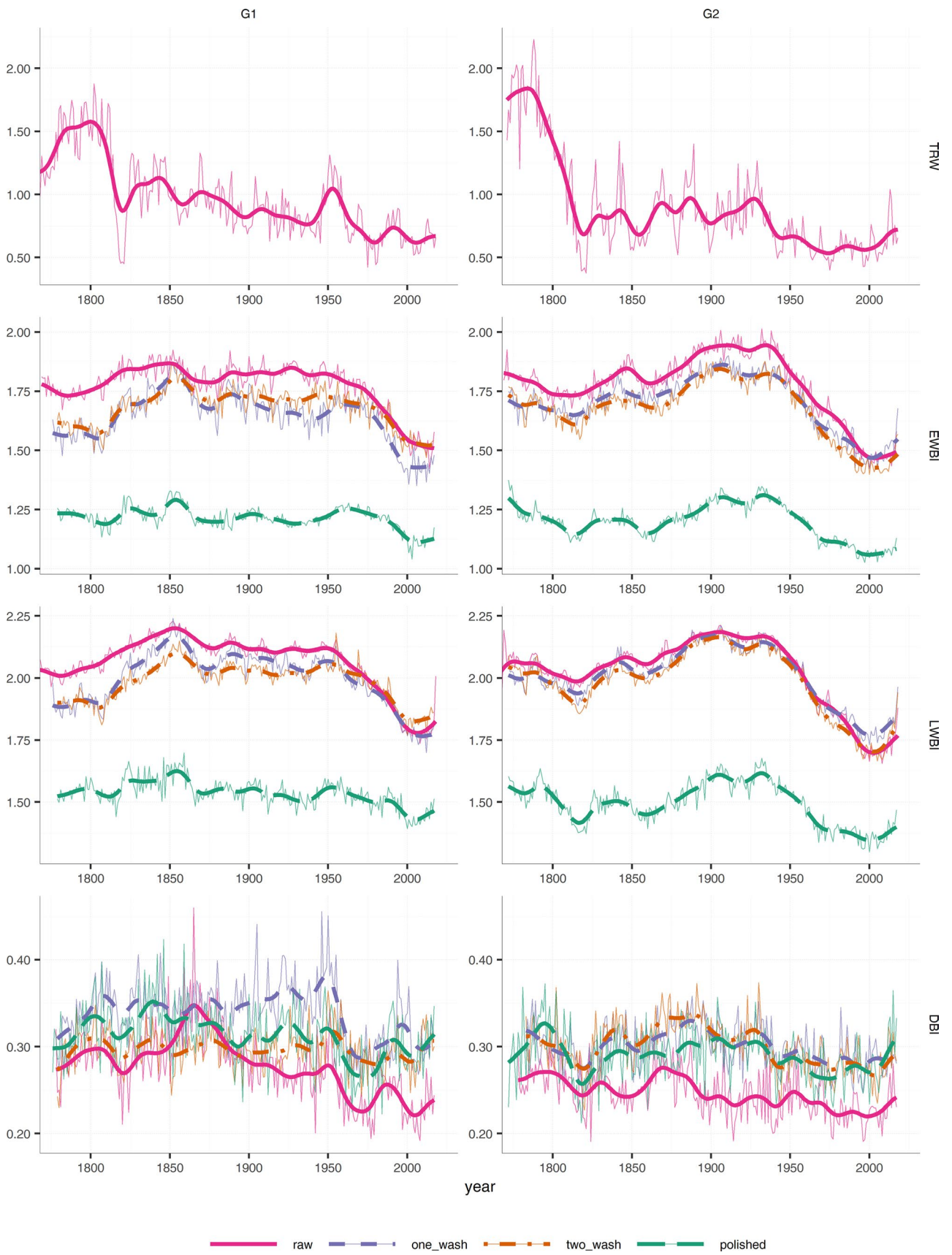




**Fig. 3** Mean BI chronologies (EWBI, LWBI, and DBI). Thick lines represent the trend of the mean series obtained by applying a 30-year, low-pass, Gaussian filter. Raw TRW chronologies are added for comparison. Note that the y-axes are scaled differently

Since this is a preliminary study with a rather small number of samples coming from a single valley in the Ortles-Cevedale Group (Italian Alps), our results could vary if a larger dataset and/or other areas along the Alpine Arch were considered.

## BI datasets

Our results showed that the percentage of considered pixels inside the frame only slightly affected the final values and their statistical parameters, especially in the washed and polished series. Considering a minor percentage of pixels, the EWBI values tended to be lower, and the LWBI values were higher (Fig. S4 in the Supplementary Material). Therefore, the rise in the considered percentage of pixels for calculation of the mean BI values tended to shift the results towards a central value, even if EWBI and LWBI were kept clearly separated. Therefore, considering the span between the first and fourth quartiles, the percentage of selected pixels inside each frame seemed to have minor importance for the final series. This was also confirmed by the limited standard deviations reported by different chronologies and the high correlation values calculated among them (not shown).

Unlike other species in the Alps (Österreicher et al. 2014), in Swiss stone pine, the distribution of the BI values was far from being normally distributed. This deviation could be partly associated with the extractives and partly with the colour difference between sapwood and heartwood, which was only partially attenuated, despite washing in a Soxhlet apparatus (Fig. 3, and Fig. S2 in the Supplementary Material). Nonetheless, sample treatment with solvents seemed to induce an influence on the BI value, especially on the EWBI, using either ethanol or acetone. However, the type of solvent did not play a key role since the EWBI and LWBI values obtained from the samples washed with ethanol were not significantly different from the BI values obtained from samples washed with acetone in most cases (Figs. 2 and 3). The only exception was represented by the heartwood EWBI, for which the difference between G1 and G2 was significant at the 0.01 level, indicating that extraction performed using acetone made the EW more reflective than using ethanol. The same results were obtained when also considering the DBI values of heartwood and sapwood, with the DBI of G2 reporting statistically higher values than G1. However, the BI values of G1 and G2 obtained with the second wash had a similar distribution and were not as different compared to the values obtained with a single wash (Fig. 3, Table S1 in the Supplementary Material). A significantly different mean (at

the 0.05 level) between G1 and G2 was observed when only considering the two\_wash sapwood EWBI (not shown). The employment of different solvents and protocols has provided different results for other species (Rydval et al. 2014). The limited number of differences considering EWBI and LWBI values in this study was probably related to the use of both solvents in a Soxhlet apparatus, whereas the significant difference highlighted in DBI was probably due to the higher degree-of-freedom and the lower variance shown by these datasets compared to EWBI and LWBI datasets, since the absolute difference in DBI values was completely comparable with values obtained by EWBI and LWBI. Therefore, there seems to be no reason to prefer ethanol over acetone or vice versa; however, different results may have been derived with a higher number of samples. We must note that sample thickness might influence the effectiveness of the extraction even if previously used thick samples showed no relevant issues (Campbell et al. 2011). However, a precise understanding of the relations occurring between solvents, washing time, and core diameter is beyond the aim of this work; therefore, specifically designed experiments will be necessary to disentangle these aspects.

The polishing procedure had a stronger impact than the solvents on the BI value (Fig. 3). A limited number of studies have used a microtome to prepare flat sample surfaces and have reported the lack of wood dust as a possible source of shade effect in the open tracheid or a diminished visibility of the ring boundaries (Österreicher et al. 2014; Frank and Nicolussi 2020). In our study, these issues were also found in Swiss stone pine. Raw and washed chronologies showed much higher BI values than polished chronologies (Fig. 3), i.e., a lower digital number in the blue band of the images and more difficulties in distinguishing ring boundaries on scanned images. Moreover, polishing of the sample entailed partial attenuation of the sapwood discoloration effect (Fig. 3). Indeed, a sudden decrease in the BI values observed at the sapwood/heartwood transition was attenuated by polishing and even more by DBI calculation (Björklund et al. 2014).

Usually, when a microtome is used to prepare samples, the tracheid will be filled with chalk to increase the contrast of the measurement and avoid shade effects (Österreicher et al. 2014; Frank and Nicolussi 2020). However, the creation of datasets from the same samples involving unfilled and filled tracheids permits us to tentatively test whether the BI value variation is a function of the lignin content or cell-wall thickness. In the first case, the two\_wash dataset should have higher  $r_{bt}$  and EPS values and correlate with climate, compared to the polished dataset, since the BI values were not affected by the wood dust coming from other rings (and thus contaminated with lignin from other rings). In contrast, if BI value variations are more dependent on the cell-wall dimensions, polished BI values should have higher

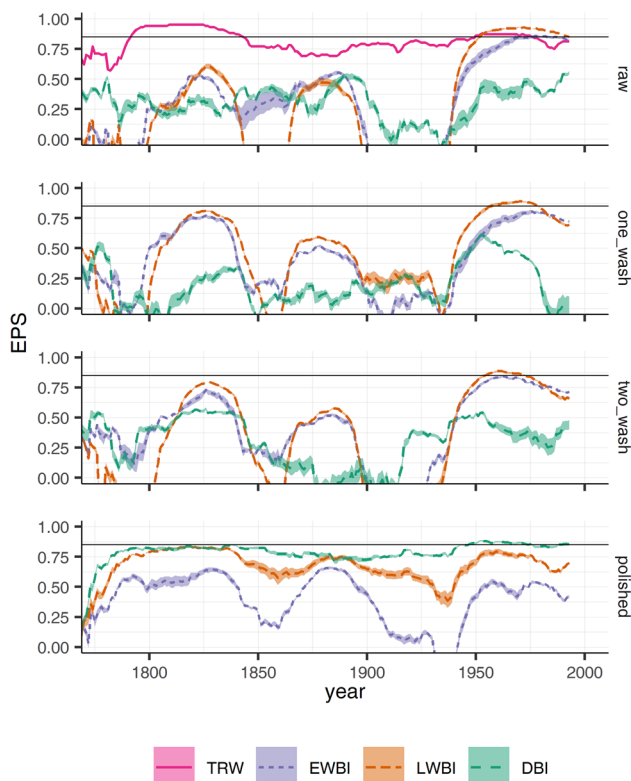


**Fig. 4** EPS values of EWBI, LWBI and DBI for raw, one\_wash, two\_wash and polished treatments (G1 and G2 aggregated). Horizontal solid lines represent EPS values equal to 0.85. TRW EPS for comparison

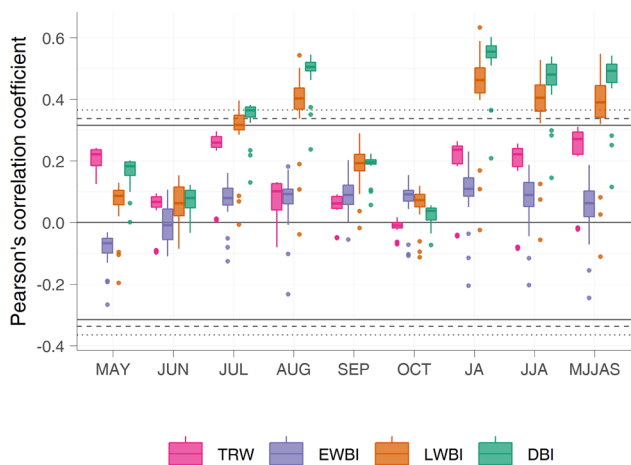


**Fig. 5** Boxplot of the correlation values between polished BI chronologies (G1 and G2 aggregated) and temperature data (i.e., monthly mean minimum, mean, and mean maximum temperature). The boxes identify the distribution of the correlation values of all considered polished chronologies (all pixel percentages and detrends) with all considered temperature data (minimum, mean and maximum). Dots represent outliers in the correlation value distribution. Solid, dashed, and dotted lines represent the Bonferroni corrected p-values at significance levels of 95%, 99% and 99.9%, respectively. TRW correlation for comparison

**Table 2** Correlation values between polished DBI datasets (i.e., all considered pixel percentages) standardized with a flexible spline (50% variance cut-off at 30 years) and temperature datasets

	Temp [ $r \pm 10^{-3}$ ]	Temp_Max [ $r \pm 10^{-3}$ ]	Temp_Min [ $r \pm 10^{-3}$ ]
Jul	$0.36 \pm 3$	$0.36 \pm 3$	$0.34 \pm 2$
	<i><math>0.23 \pm 5</math></i>	<i><math>0.23 \pm 4</math></i>	<i><math>0.21 \pm 3</math></i>
	<u><math>0.48 \pm 3</math></u>	<u><math>0.48 \pm 3</math></u>	<u><math>0.46 \pm 3</math></u>
Aug	$0.50 \pm 7$	$0.53 \pm 8$	$0.52 \pm 6$
	<i><math>0.39 \pm 8</math></i>	<i><math>0.43 \pm 9</math></i>	<i><math>0.42 \pm 5</math></i>
	<u><math>0.60 \pm 6</math></u>	<u><math>0.63 \pm 7</math></u>	<u><math>0.61 \pm 5</math></u>
JA	$0.57 \pm 5$	$0.60 \pm 6$	$0.55 \pm 5$
	<i><math>0.47 \pm 7</math></i>	<i><math>0.50 \pm 8</math></i>	<i><math>0.45 \pm 4</math></i>
	<u><math>0.65 \pm 4</math></u>	<u><math>0.69 \pm 5</math></u>	<u><math>0.64 \pm 4</math></u>
JJA	$0.50 \pm 6$	$0.51 \pm 8$	$0.45 \pm 5$
	<i><math>0.38 \pm 8</math></i>	<i><math>0.41 \pm 10</math></i>	<i><math>0.33 \pm 4</math></i>
	<u><math>0.59 \pm 5</math></u>	<u><math>0.61 \pm 7</math></u>	<u><math>0.54 \pm 4</math></u>
MJJAS	$0.51 \pm 5$	$0.53 \pm 7$	$0.48 \pm 4$
	<i><math>0.40 \pm 6</math></i>	<i><math>0.43 \pm 9</math></i>	<i><math>0.37 \pm 3</math></i>
	<u><math>0.60 \pm 4</math></u>	<u><math>0.62 \pm 6</math></u>	<u><math>0.57 \pm 3</math></u>

Uncertainties identify the confidence interval at 95% of the correlation results with different BI datasets. Italics: lower level of the confidence interval at 95% of bootstrap results; and Underlining: upper level of the confidence interval at 95% of bootstrap results

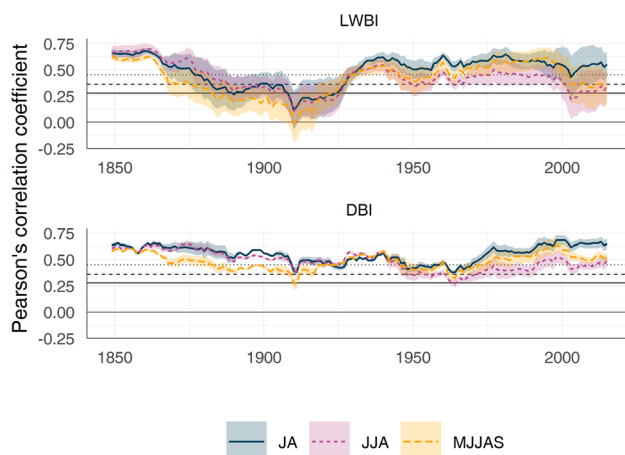


**Fig. 6** Moving correlation values between mean maximum temperature (aggregated JA, JJA and MJJAS) and both LWBI- and DBI-polished chronologies (G1 and G2 aggregated). Lines represent the mean correlation, while shaded areas represent one standard deviation around the mean. Horizontal solid, dashed, and dotted lines represent the p-values at significance levels of 95%, 99% and 99.9%, respectively

EPS and climate association due to the refined extraction of relative wood density (Björklund et al. 2021), which is based on cell-wall area divided by total cell area. Comparing the  $r_{bt}$  and EPS values obtained by the two\_wash and polished datasets (Table 1), it is clear that both parameters were

higher in the latter dataset. Moreover, the variance of the considered parameters was also much lower in the polished dataset compared to the two\_wash dataset (in general, by one order of magnitude). Regarding the correlation with climate, considering only the aggregated JA mean maximum temperature (more details on this are reported in the following paragraph), the coefficients were  $0.51 \pm 0.15$  and  $0.15 \pm 0.07$  for the polished and two\_wash datasets, respectively (EWBI, LWBI and DBI were bulked for brevity). These results corroborate the hypothesis that BI variation is driven by the cell-wall dimension rather than the cell lignin content in Swiss stone pine, as well as in the already analysed species (Björklund et al. 2021). Moreover, the obtained results highlight the need to polish or fill fibre voids with chalk to emphasize the relative density in latewood and improve the quality of the retrieved information (Fig. 4; Table 1) and thus to obtain a more suitable proxy for climate investigations.

### BI–climate correlation

Considering the polished chronologies, only LWBI and DBI were highly correlated with temperature, whereas EWBI did not seem to be influenced by this climatic factor. However, precipitation seemed to have no effect on the Swiss stone pine tree-ring features. The highest correlations with temperature were calculated between the polished BI chronologies and the aggregated temperatures in July and August (Fig. 5). This is a shorter time window compared to what was obtained with the density analysis performed on the same species (Cerrato et al. 2019b). A 5 month window featured the best results between MXD and temperature, but these were not in contradiction since high correlation values could also be observed with mean temperatures in July and August (Fig. S6 in the Supplementary Material) (Cerrato et al. 2019b). The BI data, on the other hand, could be compared with wood anatomical traits, especially when considering the association between latewood cell-wall thickness and temperature (Carrer et al. 2018). This corroborates the idea that the Swiss stone pine BI could be used as an inexpensive and time-saving proxy for wood density and thus for cell-wall thickness (Björklund et al. 2021). As theorized and discussed for Scots pine (Björklund et al. 2014), the Swiss stone pine DBI and LWBI were also consistent with the cell-wall thickness series, which could currently be considered the parameter better able to represent relative density (Björklund et al. 2021). In addition, the absence of an evident decrease in correlation during years characterized by massive larch budmoth outbreaks in the study area (Cerrato et al. 2019a) highlights the potential of this proxy to improve climatic reconstructions mainly based on larch series. Considering the mid- and low-frequencies (more than a 16-year period, sensu Melvin 2004), the representativeness of the LWBI chronologies becomes more questionable (details

about this analysis are reported in the Supplementary Material). Issues between BI and low frequencies have already been reported for Scots pine (*Pinus sylvestris* L.) (Rydval et al. 2014) and Engelmann spruce (*Picea engelmannii* Parry ex Engelm.) (Wilson et al. 2014) and were solved by using BI-adjusted values (Björklund et al. 2014, 2015; Fuentes et al. 2018). The optimal application of this correction technique requires parallel BI and density measurements that were unavailable at the time of this study. However, making this effort in the future should still be considered, owing to the high correlation and the high power-spectrum values obtained in the high-frequency domain, even if the latter are not continuously statistically significant (Fig. S7 in the Supplementary Material). The lack of a significant correlation with precipitation is consistent with a number of recent studies. These studies involved other physical tree-ring parameters possibly associated with BI (i.e., maximum wood density and cell-wall thickness) and reported no correlation with precipitation (Cerrato et al. 2019b) or slightly significant values related to earlywood cell-wall parameters (Carrer et al. 2018).

The potential of the Swiss stone pine BI data as a proxy for summer temperature was also confirmed by the stability of the signal recorded by moving correlation analysis (Fig. 6). The moving correlation analysis showed a stable significant correlation with JA mean maximum temperature for almost all the 1800–2017 period. Higher correlation values between TRW and mean monthly maximum temperature rather than mean or mean minimum temperature have already been observed in the Alps (Carrer et al. 1998; Carrer and Urbinati 2004). The slight shift in the significant monthly association was probably caused by the wider significant climate window in which blue intensity was able to record in comparison to TRW. Moreover, the MXD response was higher for the mean maximum temperature compared to the mean minimum and mean temperatures (not shown). Better performance in the correlation with mean maximum temperature, compared with mean minimum or mean temperature, is due to the main importance of the former parameter as a limiting factor for growth, more than the latter (Carrer et al. 1998; Carrer and Urbinati 2004).

An interesting pattern emerged when considering the correlation values obtained between BI chronologies and MJJAS aggregated mean maximum temperatures compared to the correlation values obtained with the JJA aggregated mean maximum temperature (Fig. 6). In fact, the former returned stable values until the 1960s, followed by a slightly increasing trend, whereas the latter showed a modest decreasing trend since the 1850s for the entire analysed time period. This different behaviour shown by the temperature correlation values of MJJAS with respect to JJA might represent a sensitivity shift of Swiss stone pine caused by increasing temperatures at the site altitude, as also reported

for high-latitude sites (Linderholm 2006; Schwab et al. 2018). It has indeed been demonstrated that it is the time duration of woody material deposition that mostly influences the cell-wall thickness of conifers living in cold climates (Uggla 2001; Rossi et al. 2006; Carrer et al. 2018). It has been argued that higher temperatures during the early and late periods of the growing season can lead to the production and deposition of more cell-wall compounds (Carrer et al. 2007; Saulnier et al. 2011). The same effect can be observed in the maximum latewood density (Cerrato et al. 2019b) but not in the TRW data (Leonelli et al. 2011), where it has been demonstrated that the TRW–temperature relationship remains stable over time despite the elongation of the thermal growing season (Stridbeck et al. 2022). An alternative explanation for this peculiar pattern can be found in the heartwood–sapwood transition; starting from the 1930s, decreasing BI values can be observed in the EWBI and LWBI chronologies (Fig. 3). Although the long-term trend was removed by standardization, the heartwood–sapwood transition effect could still affect the high-frequency signal with a magnitude that is a function of the stiffness of the standardization method. However, the permanence of trends also in the correlation values of the DBI chronologies with almost the same intensity as that in the LWBI chronologies led to the suggestion that the pattern could be attributed to climate change affecting high-altitude areas with major intensity (Intergovernmental Panel on Climate Change (IPCC) 2022), more than to the transition effect.

The correlation between the BI and monthly aggregated JA temperatures did not show a decrease in the correlation values in the most recent decades and did not seem to be affected by the so-called divergence problem (Büntgen et al. 2008; D'Arrigo et al. 2008; Coppola et al. 2012), as reported also for the Swiss stone pine MXD standard chronology in the area (Cerrato et al. 2019b, 2020) or other species TRW standard chronologies in the Alps (Leonelli et al. 2016). Considering the similarity of the values obtained from the correlation of both the DBI and MXD chronologies with temperature (Fig. S6 in the Supplementary Material), the limited standard deviation obtained by different DBI chronologies (considering different percentages of pixels and different standardization methods), and the similarity in the frequency response of these proxies to temperature (Figs. S7 and S8 in the Supplementary Material), BI could be considered a potential alternative to MXD, at least in the study area.

## Conclusions

Our results highlight the possibility of using BI, and especially DBI, in Swiss stone pine as a better proxy parameter than TRW. Considering the mid- and low-frequencies,

some issues still exist and deserve more detailed investigation and specific approaches (e.g., thinner samples, different discolouration treatments, and different standardization and/or data adjustment). Ethanol and acetone affected the final results similarly; therefore, there is no reason to prefer one solvent over the other, as long as the samples are washed in a Soxhlet apparatus for at least 72 h. On the other hand, the polishing process strongly influenced the final values. This approach is strongly recommended before scanning the samples, since the identification of ring borders is easier in a polished sample and permits us to obtain better information about the relative wood density, which returns the highest correlation values with temperature. The obtained results corroborate the hypothesis that the cell-wall dimension rather than lignin content also drives BI variation in Swiss stone pine. The setting frame for calculation of the BI values had a marginal effect on the results, especially if we consider the DBI values; however, the lower the considered percentile of pixels was, the higher the variance of the series obtained. Therefore, to avoid the creation of Swiss stone pine BI series characterized by an artificial method-induced variance, at least 25% of the pixels in the BI frame should be considered.

Dendroclimatic analysis shows that, unlike MXD, Swiss stone pine DBIs are sensitive to a shorter summer temperature window (JA). These discrepancies can be ascribable to the difference that characterize the two proxies, but also to the different resolution to which the MXD and the DBIs are measured. The lower resolution with which the DBIs may be measured could make the obtained data more similar to ring-width data than to MXD. However, these properties must be considered, especially when combined proxies involving different methods are used for climatic reconstruction.

These results supply some preliminary information about blue intensity applied to Swiss stone pine in the Alps, and they open new perspectives on this overlooked species. The immunity of Swiss stone pine from any significant insect defoliator outbreaks also makes this proxy particularly suitable to reconstruct past high-frequency temperature variation. Thus, Swiss stone pine deserves further investigation and attention if we want to fully appreciate the climate-proxy potential of this species also considering that the comparison between Swiss stone pine BI data and data obtained by European larch can open new perspectives to both investigate historical defoliator attacks, and to more robustly correct and reconstruct climate.

**Supplementary Information** The online version contains supplementary material available at <https://doi.org/10.1007/s10342-023-01566-9>.

**Acknowledgements** This research was supported by the Laboratory of dendrochronology of the Department of Earth Science (University of Pisa, Fondi Ateneo 2017–2019, C. Baroni and M.C. Salvatore) and by the project of strategic interest NEXTDATA (PNR National Research Programme 2011–2013; project coordinator A. Provenzale CNR-IGG, WP 1.6, leader C. Baroni UNIPI and CNR-IGG). We thank

the Editor Prof. Ruediger Grote, Dr. Jesper Björklund, and an anonymous reviewer, for their constructive comments and suggestions, which allowed to improve the manuscript.

**Author contributions** Project design by RC, CB and MCS. Climatic dataset were processed by MB, RC. prepared the first draft of the manuscript, the final version being accomplished with contribute from RC, CB, MCS, MB and MC. CB and MCS provided the funding.

**Funding** Open access funding provided by Università di Pisa within the CRUI-CARE Agreement. This work was financially supported by the University of Pisa (Fondi Ateneo 2017–2019, C. Baroni and M.C. Salvatore) and project of strategic interest NEXTDATA (PNR National Research Programme 2011–2013; project coordinator A. Provenzale CNR-IGG, WP 1.6, leader C. Baroni UNIPI and CNR-IGG).

**Data Availability** Not applicable.

## Declarations

**Competing interests** The authors declare no competing interests.

**Conflict of interest** Any use of trade, firm, or product names is for descriptive purposes only and does not imply endorsement by the involved universities. The authors declare that they have no conflicts of interest.

**Open Access** This article is licensed under a Creative Commons Attribution 4.0 International License, which permits use, sharing, adaptation, distribution and reproduction in any medium or format, as long as you give appropriate credit to the original author(s) and the source, provide a link to the Creative Commons licence, and indicate if changes were made. The images or other third party material in this article are included in the article's Creative Commons licence, unless indicated otherwise in a credit line to the material. If material is not included in the article's Creative Commons licence and your intended use is not permitted by statutory regulation or exceeds the permitted use, you will need to obtain permission directly from the copyright holder. To view a copy of this licence, visit <http://creativecommons.org/licenses/by/4.0/>.

## References

- Anchukaitis KJ, Wilson R, Briffa KR et al (2017) Last millennium Northern Hemisphere summer temperatures from tree rings: part II, spatially resolved reconstructions. *Quat Sci Rev* 163:1–22. <https://doi.org/10.1016/j.quascirev.2017.02.020>
- Andreis C, Armiraglio S, Caccianiga M et al (2005) Pinus Cembra L. nel settore sud-Alpino Lombardo (Italia Settentrionale). *Nat Brescia - Ann Mus Civ Sc Nat, Brescia* 34:19–39
- Arbellay E, Jarvis I, Chavardès RD et al (2018) Tree-ring proxies of larch bud moth defoliation: latewood width and blue intensity are more precise than tree-ring width. *Tree Physiol* 38:1237–1245. <https://doi.org/10.1093/treephys/tpy057>
- Babst F, Wright WE, Szejner P et al (2016) Blue intensity parameters derived from Ponderosa pine tree rings characterize intra-annual density fluctuations and reveal seasonally divergent water limitations. *Trees Struct Funct* 30:1403–1415. <https://doi.org/10.1007/s00468-016-1377-6>
- Baltensweiler W, Fischlin A (1988) The larch budmoth in the alps. In: Berryman AA (ed) *Dynamics of Forest Insect Populations*. Springer, US, Boston, MA, pp 331–351
- Björklund J, Gunnarson BE, Seftigen K et al (2014) Blue intensity and density from northern Fennoscandian tree rings, exploring the potential to improve summer temperature reconstructions with earlywood information. *Clim past* 10:877–885. <https://doi.org/10.5194/cp-10-877-2014>
- Björklund J, Gunnarson BE, Seftigen K et al (2015) Using adjusted Blue Intensity data to attain high-quality summer temperature information: a case study from Central Scandinavia. *Holocene* 25:547–556. <https://doi.org/10.1177/0959683614562434>
- Björklund J, von Arx G, Nievergelt D et al (2019) Scientific merits and analytical challenges of tree-ring densitometry. *Rev Geophys* 57:1224–1264. <https://doi.org/10.1029/2019RG000642>
- Björklund J, Seftigen K, Fonti P et al (2020) Dendroclimatic potential of dendroanatomy in temperature-sensitive Pinus sylvestris. *Dendrochronologia* 60:125673. <https://doi.org/10.1016/j.dendro.2020.125673>
- Björklund J, Fonti MV, Fonti P et al (2021) Cell wall dimensions reign supreme: cell wall composition is irrelevant for the temperature signal of latewood density/blue intensity in Scots pine. *Dendrochronologia* 65:125785. <https://doi.org/10.1016/j.dendro.2020.125785>
- Blake SAP, Palmer JG, Björklund J et al (2020) Palaeoclimate potential of New Zealand *Manoao colensoi* (silver pine) tree rings using Blue-Intensity (BI). *Dendrochronologia* 60:125664. <https://doi.org/10.1016/j.dendro.2020.125664>
- Boninsegna JA, Argollo J, Aravena JC et al (2009) Dendroclimatic reconstructions in South America: a review. *Palaeogeogr Palaeoclimatol Palaeoecol* 281:210–228. <https://doi.org/10.1016/j.palaeo.2009.07.020>
- Briffa KR (2000) Annual climate variability in the Holocene: interpreting the message of ancient trees. *Quat Sci Rev* 19:87–105. [https://doi.org/10.1016/S0277-3791\(99\)00056-6](https://doi.org/10.1016/S0277-3791(99)00056-6)
- Brookhouse M, Graham R (2016) Application of the minimum blue-intensity technique to a Southern-hemisphere conifer. *Tree-Ring Res* 72:103–107. <https://doi.org/10.3959/1536-1098-72.02.103>
- Brunetti M, Lentini G, Maugeri M et al (2012) Projecting North Eastern Italy temperature and precipitation secular records onto a high-resolution grid. *Phys Chem Earth parts a/b/c* 40–41:9–22. <https://doi.org/10.1016/j.pce.2009.12.005>
- Buckley BM, Hansen KG, Griffin KL et al (2018) Blue intensity from a tropical conifer's annual rings for climate reconstruction: an eco-physiological perspective. *Dendrochronologia* 50:10–22. <https://doi.org/10.1016/j.dendro.2018.04.003>
- Bunn AG (2008) A dendrochronology program library in R (dplR). *Dendrochronologia* 26:115–124. <https://doi.org/10.1016/j.dendro.2008.01.002>
- Büntgen U, Esper J, Frank DC et al (2005) A 1052-year tree-ring proxy for Alpine summer temperatures. *Clim Dyn* 25:141–153. <https://doi.org/10.1007/s00382-005-0028-1>
- Büntgen U, Frank DC, Nievergelt D, Esper J (2006) Summer temperature variations in the European Alps, A.D. 755–2004. *J Clim* 19:5606–5623. <https://doi.org/10.1175/JCLI3917.1>
- Büntgen U, Frank DC, Wilson R et al (2008) Testing for tree-ring divergence in the European Alps. *Glob Chang Biol* 14:2443–2453. <https://doi.org/10.1111/j.1365-2486.2008.01640.x>
- Büntgen U, Frank DC, Liebhold AM et al (2009) Three centuries of insect outbreaks across the European Alps. *New Phytol* 182:929–941. <https://doi.org/10.1111/j.1469-8137.2009.02825.x>
- Büntgen U, Tegel W, Nicolussi K et al (2011) 2500 years of European climate variability and human susceptibility. *Science* 331:578–582. <https://doi.org/10.1126/science.1197175>
- Büntgen U, Liebhold A, Nievergelt D et al (2020) Return of the moth: rethinking the effect of climate on insect outbreaks. *Oecologia* 192:543–552. <https://doi.org/10.1007/s00442-019-04585-9>
- Buras A (2017) A comment on the expressed population signal. *Dendrochronologia* 44:130–132. <https://doi.org/10.1016/j.dendro.2017.03.005>

- Buras A, Spyt B, Janecka K, Kaczka RJ (2018) Divergent growth of Norway spruce on Babia Góra Mountain in the western Carpathians. *Dendrochronologia* 50:33–43. <https://doi.org/10.1016/j.dendro.2018.04.005>
- Campbell R, McCarroll D, Loader NJ et al (2007) Blue intensity in *Pinus sylvestris* tree-rings: developing a new palaeoclimate proxy. *Holocene* 17:821–828. <https://doi.org/10.1177/0959683607080523>
- Campbell R, McCarroll D, Robertson I et al (2011) Blue intensity in *Pinus sylvestris* tree rings: a manual for a new palaeoclimate proxy. *Tree-Ring Res* 67:127–134. <https://doi.org/10.3959/2010-13.1>
- Cao X, Fang K, Chen P et al (2020) Microdensitometric records from humid subtropical China show distinct climate signals in earlywood and latewood. *Dendrochronologia*. <https://doi.org/10.1016/j.dendro.2020.125764>
- Carrer M, Urbinati C (2004) Age-dependent tree-ring growth responses to climate in *Larix decidua* and *Pinus cembra*. *Ecology* 85:730–740. <https://doi.org/10.1890/02-0478>
- Carrer M, Anfodillo T, Urbinati C, Carraro V (1998) High-altitude forest sensitivity to global warming: results from long-term and short-term analyses in the eastern Italian Alps. In: Beniston M, Innes JL (eds) *The Impacts of Climate Variability on Forests*. Springer, Verlag Berlin Heidelberg, pp 171–189
- Carrer M, Nola P, Edouard J-L et al (2007) Regional variability of climate growth relationships in *Pinus cembra* high elevation forests in the Alps. *J Ecol* 95:1072–1083. <https://doi.org/10.1111/j.1365-2745.2007.01281.x>
- Carrer M, Unterholzner L, Castagneri D (2018) Wood anatomical traits highlight complex temperature influence on *Pinus cembra* at high elevation in the Eastern Alps. *Int J Biometeorol* 62:1745–1753. <https://doi.org/10.1007/s00484-018-1577-4>
- Carturan L, Dalla Fontana G, Borga M (2012) Estimation of winter precipitation in a high-altitude catchment of the Eastern Italian Alps: validation by means of glacier mass balance observations. *Geogr Fis e Din Quat* 35:37–48. <https://doi.org/10.4461/GFDQ.2012.35.4>
- Cerrato R, Salvatore MC, Brunetti M et al (2018) Dendroclimatic relevance of “Bosco Antico”, the most ancient living European larch wood in the Southern Rhaetian Alps (Italy). *Geogr Fis e Din Quat* 41:35–49. <https://doi.org/10.4461/GFDQ.2018.41.3>
- Cerrato R, Cherubini P, Büntgen U et al (2019a) Tree-ring-based reconstruction of larch budmoth outbreaks in the Central Italian Alps since 1774 CE. *iForest Biogeosci* 12:289–296. <https://doi.org/10.3832/ifor2533-012>
- Cerrato R, Salvatore MC, Gunnarson BE et al (2019b) A *Pinus cembra* L. tree-ring record for late spring to late summer temperature in the Rhaetian Alps. *Italy Dendrochronologia* 53:22–31. <https://doi.org/10.1016/j.dendro.2018.10.010>
- Cerrato R, Salvatore MC, Gunnarson BE et al (2020) *Pinus cembra* L. tree-ring data as a proxy for summer mass-balance variability of the Careser Glacier (Italian Rhaetian Alps). *J Glaciol* 66:714–726. <https://doi.org/10.1017/jog.2020.40>
- Cleaveland MK, Stahle DW, Therrell MD et al (2003) Tree-ring reconstructed winter precipitation and tropical teleconnections in Durango, Mexico. *Clim Change* 59:369–388. <https://doi.org/10.1023/A:1024835630188>
- Coppola A, Leonelli G, Salvatore MC et al (2012) Weakening climatic signal since mid-20th century in European larch tree-ring chronologies at different altitudes from the Adamello-Presanella Massif (Italian Alps). *Quat Res* 77:344–354. <https://doi.org/10.1016/j.yqres.2012.01.004>
- Corona C, Guiot J, Edouard J-L et al (2010) Millennium-long summer temperature variations in the European Alps as reconstructed from tree rings. *Clim past* 6:379–400. <https://doi.org/10.5194/cp-6-379-2010>
- Corona C, Edouard J-L, Guibal F et al (2011) Long-term summer (AD751–2008) temperature fluctuation in the French Alps based on tree-ring data. *Boreas* 40:351–366. <https://doi.org/10.1111/j.1502-3885.2010.00185.x>
- Crespi A, Brunetti M, Lentini G, Maugeri M (2018) 1961–1990 high-resolution monthly precipitation climatologies for Italy. *Int J Climatol* 38:878–895. <https://doi.org/10.1002/joc.5217>
- D’Arrigo RD, Wilson R, Liepert B, Cherubini P (2008) On the “Divergence Problem” in Northern Forests: a review of the tree-ring evidence and possible causes. *Glob Planet Change* 60:289–305. <https://doi.org/10.1016/j.gloplacha.2007.03.004>
- Dannenber MP, Wise EK (2016) Seasonal climate signals from multiple tree ring metrics: a case study of *Pinus ponderosa* in the upper Columbia River Basin. *J Geophys Res Biogeosciences* 121:1178–1189. <https://doi.org/10.1002/2015JG003155>
- Davi NK, Rao MP, Wilson R et al (2021) Accelerated recent warming and temperature variability over the past eight centuries in the Central Asian Altai from blue intensity in tree rings. *Geophys Res Lett*. <https://doi.org/10.1029/2021GL092933>
- Dolgova E (2016) June–September temperature reconstruction in the Northern Caucasus based on blue intensity data. *Dendrochronologia* 39:17–23. <https://doi.org/10.1016/j.dendro.2016.03.002>
- Esper J, Büntgen U, Frank DC et al (2007) 1200 Years of regular outbreaks in alpine insects. *Proc R Soc B Biol Sci* 274:671–679. <https://doi.org/10.1098/rspb.2006.0191>
- Esper J, Schneider L, Smerdon JE et al (2015) Signals and memory in tree-ring width and density data. *Dendrochronologia* 35:62–72. <https://doi.org/10.1016/j.dendro.2015.07.001>
- Esper J, George SS, Anchukaitis K et al (2018) Large-scale, millennial-length temperature reconstructions from tree-rings. *Dendrochronologia* 50:81–90. <https://doi.org/10.1016/j.dendro.2018.06.001>
- Frank T, Nicolussi K (2020) Testing different Earlywood/Latewood delimitations for the establishment of Blue Intensity data: a case study based on Alpine *Picea abies* samples. *Dendrochronologia* 64:125775. <https://doi.org/10.1016/j.dendro.2020.125775>
- Fritts HC (ed) (1976). Elsevier, London
- Fuentes M, Salo R, Björklund J et al (2018) A 970-year-long summer temperature reconstruction from Rogen, west-central Sweden, based on blue intensity from tree rings. *Holocene* 28:254–266. <https://doi.org/10.1177/0959683617721322>
- Galvan P, Ponge J-F, Chersich S, Zanella A (2008) Humus components and soil biogenic structures in Norway spruce ecosystems. *Soil Sci Soc Am J* 72:548. <https://doi.org/10.2136/sssaj2006.0317>
- Gentili R, Armiraglio S, Sgorbati S, Baroni C (2013) Geomorphological disturbance affects ecological driving forces and plant turnover along an altitudinal stress gradient on alpine slopes. *Plant Ecol* 214:571–586. <https://doi.org/10.1007/s11258-013-0190-1>
- Gentili R, Baroni C, Panigada C et al (2020) Glacier shrinkage and slope processes create habitat at high elevation and microrefugia across treeline for alpine plants during warm stages. *CATENA* 193:104626. <https://doi.org/10.1016/j.catena.2020.104626>
- Granato-Souza D, Stahle DW, Barbosa AC et al (2019) Tree rings and rainfall in the equatorial Amazon. *Clim Dyn* 52:1857–1869. <https://doi.org/10.1007/s00382-018-4227-y>
- Heeter KJ, Harley GL, Van De Gevel SL, White PB (2019) Blue intensity as a temperature proxy in the eastern United States: a pilot study from a southern disjunct population of *Picea rubens* (Sarg.). *Dendrochronologia* 55:105–109. <https://doi.org/10.1016/j.dendro.2019.04.010>
- Heeter KJ, Harley GL, Maxwell JT et al (2020) Late summer temperature variability for the Southern Rocky Mountains (USA) since 1735 CE: applying blue light intensity to low-latitude

- Picea engelmannii* Parry ex Engelm. *Clim Change* 162:965–988. <https://doi.org/10.1007/s10584-020-02772-9>
- Holmes RL (1983) Computer-assisted quality control in tree-ring dating and measurement. *Tree-Ring Bull* 43:69–78. <https://doi.org/10.1016/j.ecoleng.2008.01.004>
- Immerzeel WW, Lutz AF, Andrade M et al (2020) Importance and vulnerability of the world's water towers. *Nature* 577:364–369. <https://doi.org/10.1038/s41586-019-1822-y>
- Intergovernmental Panel on Climate Change (IPCC) (2022) The ocean and cryosphere in a changing climate. Cambridge University Press, Principality of Monaco
- Isotta FA, Frei C, Weigluni V et al (2014) The climate of daily precipitation in the Alps: development and analysis of a high-resolution grid dataset from pan-Alpine rain-gauge data. *Int J Climatol* 34:1657–1675. <https://doi.org/10.1002/joc.3794>
- IUSS Working Group (2007) Technical Report 103. Rome
- Kaczka RJ, Spyt B, Janecka K et al (2018) Different maximum latewood density and blue intensity measurements techniques reveal similar results. *Dendrochronologia* 49:94–101. <https://doi.org/10.1016/j.dendro.2018.03.005>
- Leavitt SW, Roden J (2022) Stable isotopes in tree rings. Springer International Publishing, Cham
- Leonelli G, Pelfini M, D'Arrigo RD et al (2011) Non-stationary Responses of tree-ring chronologies and glacier mass balance to climate in the European Alps. *Arctic Antarct Alp Res* 43:56–65. <https://doi.org/10.1657/1938-4246-43.1.56>
- Leonelli G, Coppola A, Baroni C et al (2016) Multispecies dendroclimatic reconstructions of summer temperature in the European Alps enhanced by trees highly sensitive to temperature. *Clim Change* 137:275–291. <https://doi.org/10.1007/s10584-016-1658-5>
- Linderholm HW (2006) Growing season changes in the last century. *Agric for Meteorol* 137:1–14. <https://doi.org/10.1016/j.agrfor.2006.03.006>
- Linderholm HW, Björklund J, Seftigen K et al (2010) Dendroclimatology in Fennoscandia—from past accomplishments to future potential. *Clim past* 6:93–114. <https://doi.org/10.5194/cp-6-93-2010>
- Linderholm HW, Björklund J, Seftigen K et al (2015) Fennoscandia revisited: a spatially improved tree-ring reconstruction of summer temperatures for the last 900 years. *Clim Dyn* 45:933–947. <https://doi.org/10.1007/s00382-014-2328-9>
- Ljungqvist FC, Thejll P, Björklund J et al (2020) Assessing non-linearity in European temperature-sensitive tree-ring data. *Dendrochronologia* 59:125652. <https://doi.org/10.1016/j.dendro.2019.125652>
- Lopez-Saez J, Corona C, von Arx G et al (2023) Tree-ring anatomy of *Pinus cembra* trees opens new avenues for climate reconstructions in the European Alps. *Sci Total Environ* 855:158605. <https://doi.org/10.1016/j.scitotenv.2022.158605>
- McCarroll D, Pettigrew E, Luckman A (2002) Blue reflectance provides a surrogate for latewood density of high-latitude pine tree rings reflectance provides a surrogate for latewood of high-latitude density pine tree rings. *Arctic Antarct Alp Res* 34:450–453
- Melvin TM, Briffa KR (2008) A “signal-free” approach to dendroclimatic standardisation. *Dendrochronologia* 26:71–86. <https://doi.org/10.1016/j.dendro.2007.12.001>
- Melvin TM, Briffa KR, Nicolussi K, Grabner M (2007) Time-varying-response smoothing. *Dendrochronologia* 25:65–69. <https://doi.org/10.1016/j.dendro.2007.01.004>
- Melvin TM (2004) Historical growth rates and changing climatic sensitivity of boreal conifers. PhD dissertation, University of East Anglia
- Mitchell TD, Jones PD (2005) An improved method of constructing a database of monthly climate observations and associated high-resolution grids. *Int J Climatol* 25:693–712. <https://doi.org/10.1002/joc.1181>
- Nagavciuc V, Roibu C-C, Ionita M et al (2019) Different climate response of three tree ring proxies of *Pinus sylvestris* from the Eastern Carpathians, Romania. *Dendrochronologia* 54:56–63. <https://doi.org/10.1016/j.dendro.2019.02.007>
- Nicolussi K (1995) Jahrringe und Massenbilanz. Dendroclimatologische Rekonstruktion der Massenbilanzreihe bis zum Jahr 1400 mittels *Pinus cembra*-Reihe.pdf. *Zeitschrift Fur Gletscherkd Und Glazialgeol* 30:11–52
- Nicolussi K, Bortenschlager S, Körner C (1995) Increase in tree-ring width in subalpine *Pinus cembra* from the central Alps that may be CO<sub>2</sub>-related. *Trees* 9:181–189. <https://doi.org/10.1007/BF00195270>
- Nola P, Morales MS, Motta R, Villalba R (2006) The role of larch budmoth (*Zeiraphera diniana* Gn.) on forest succession in a larch (*Larix decidua* Mill.) and Swiss stone pine (*Pinus cembra* L.) stand in the Susa Valley (Piedmont, Italy). *Trees Struct Funct* 20:371–382. <https://doi.org/10.1007/s00468-006-0050-x>
- O'connor JA, Henley BJ, Brookhouse MT, Allen KJ (2022) Ring-width and blue-light chronologies of *Podocarpus lawrencei* from south-eastern mainland Australia reveal a regional climate signal. *Clim past* 18:2567–2581. <https://doi.org/10.5194/cp-18-2567-2022>
- Oberhuber W (2004) Influence of climate on radial growth of *Pinus cembra* within the alpine timberline ecotone. *Tree Physiol* 24:291–301. <https://doi.org/10.1093/treephys/24.3.291>
- Österreicher A, Weber G, Leuenberger M, Nicolussi K (2014) Exploring blue intensity - comparison of blue intensity and MXD data from Alpine spruce trees. *Sci Tech Rep*. <https://doi.org/10.2312/GFZ.b103-15069>
- R Core Team (2022) R: a language and environment for statistical computing. R Foundation for Statistical Computing, Vienna, Austria. <https://www.R-project.org/>
- Reid E, Wilson R (2020) Delta blue intensity vs. maximum density: a case study using *Pinus uncinata* in the Pyrenees. *Dendrochronologia* 61:125706. <https://doi.org/10.1016/j.dendro.2020.125706>
- Rossi S, Deslauriers A, Anfodillo T et al (2006) Conifers in cold environments synchronize maximum growth rate of tree-ring formation with day length. *New Phytol* 170:301–310. <https://doi.org/10.1111/j.1469-8137.2006.01660.x>
- Rydval M, Larsson LÅ, McGlynn L et al (2014) Blue intensity for dendroclimatology: Should we have the blues? Experiments from Scotland. *Dendrochronologia* 32:191–204. <https://doi.org/10.1016/j.dendro.2014.04.003>
- Rydval M, Gunnarson BE, Loader NJ et al (2017a) Spatial reconstruction of Scottish summer temperatures from tree rings. *Int J Climatol* 37:1540–1556. <https://doi.org/10.1002/joc.4796>
- Rydval M, Loader NJ, Gunnarson BE et al (2017b) Reconstructing 800 years of summer temperatures in Scotland from tree rings. *Clim Dyn* 49:2951–2974. <https://doi.org/10.1007/s00382-016-3478-8>
- Salvatore MC, Zanoner T, Baroni C et al (2015) The state of Italian glaciers: a snapshot of the 2006–2007 hydrological period. *Geogr Fis e Din Quat* 38:175–198. <https://doi.org/10.4461/GFDQ.2015.38.16>
- Saulnier M, Edouard J-L, Corona C, Guibal F (2011) Climate/growth relationships in a *Pinus cembra* high-elevation network in the Southern French Alps. *Ann for Sci* 68:189–200. <https://doi.org/10.1007/s13595-011-0020-3>
- Schneider L, Smerdon JE, Büntgen U et al (2015) Revising midlatitude summer temperatures back to A.D. 600 based on a wood density network. *Geophys Res Lett* 42:4556–4562. <https://doi.org/10.1002/2015GL063956>
- Schwab N, Kaczka RJ, Janecka K et al (2018) Climate change-induced shift of tree growth sensitivity at a central Himalayan treeline ecotone. *Forests* 9:267. <https://doi.org/10.3390/f9050267>

- Schweingruber FH (1988) Tree rings basic and applications of dendrochronology. Springer, Netherlands, Dordrecht
- Schweingruber FH (1993) Trees and wood in dendrochronology. Springer, Berlin, Heidelberg
- Seftigen K, Fuentes M, Ljungqvist FC, Björklund J (2020) Using Blue Intensity from drought-sensitive *Pinus sylvestris* in Fennoscandia to improve reconstruction of past hydroclimate variability. *Clim Dyn* 55:579–594. <https://doi.org/10.1007/s00382-020-05287-2>
- Seftigen K, Fonti MV, Luckman B et al (2022) Prospects for dendroanatomy in paleoclimatology—a case study on *Picea engelmannii* from the Canadian Rockies. *Clim past* 18:1151–1168. <https://doi.org/10.5194/cp-18-1151-2022>
- Sheppard PR, Wiedenhoef A (2007) An advancement in removing extraneous color from wood for low-magnification reflected-light image analysis of conifer tree rings. *Wood Fiber Sci* 39:173–183
- Stridbeck P, Björklund J, Fuentes M et al (2022) Partly decoupled tree-ring width and leaf phenology response to 20th century temperature change in Sweden. *Dendrochronologia*. <https://doi.org/10.1016/j.dendro.2022.125993>
- Tsvetanov N, Dolgova E, Panayotov M (2020) First measurements of Blue intensity from *Pinus peuce* and *Pinus heldreichii* tree rings and potential for climate reconstructions. *Dendrochronologia* 60:125681. <https://doi.org/10.1016/j.dendro.2020.125681>
- Uggla C (2001) Function and dynamics of auxin and carbohydrates during earlywood/latewood transition in scots pine. *PLANT Physiol* 125:2029–2039. <https://doi.org/10.1104/pp.125.4.2029>
- Wang F, Arseneault D, Boucher É et al (2020) Temperature sensitivity of blue intensity, maximum latewood density, and ring width data of living black spruce trees in the eastern Canadian taiga. *Dendrochronologia* 64:125771. <https://doi.org/10.1016/j.dendro.2020.125771>
- Wigley TML, Briffa KR, Jones PD (1984) On the average value of correlated time series, with applications in dendroclimatology and hydrometeorology. *J Clim Appl Meteorol* 23:201–213. [https://doi.org/10.1175/1520-0450\(1984\)023%3c0201:OTAVOC%3e2.0.CO;2](https://doi.org/10.1175/1520-0450(1984)023%3c0201:OTAVOC%3e2.0.CO;2)
- Wilson R, Loader NJ, Rydval M et al (2012) Reconstructing holocene climate from tree rings: the potential for a long chronology from the scottish highlands. *Holocene* 22:3–11. <https://doi.org/10.1177/0959683611405237>
- Wilson R, Rao R, Rydval M et al (2014) Blue Intensity for dendroclimatology: the BC blues: a case study from British Columbia, Canada. *Holocene* 24:1428–1438. <https://doi.org/10.1177/0959683614544051>
- Wilson R, Anchukaitis KJ, Briffa KR et al (2016) Last millennium northern hemisphere summer temperatures from tree rings: part I: the long term context. *Quat Sci Rev* 134:1–18. <https://doi.org/10.1016/j.quascirev.2015.12.005>
- Wilson R, D'Arrigo R, Andreu-Hayles L et al (2017a) Experiments based on blue intensity for reconstructing North Pacific temperatures along the Gulf of Alaska. *Clim past* 13:1007–1022. <https://doi.org/10.5194/cp-13-1007-2017>
- Wilson R, Wilson D, Rydval M et al (2017b) Facilitating tree-ring dating of historic conifer timbers using Blue Intensity. *J Archaeol Sci* 78:99–111. <https://doi.org/10.1016/j.jas.2016.11.011>
- Wilson R, Anchukaitis KJ, Andreu-Hayles L et al (2019) Improved dendroclimatic calibration using blue intensity in the southern Yukon. *The Holocene* 29:1817–1830. <https://doi.org/10.1177/0959683619862037>
- Wilson R, Allen K, Baker P et al (2021) Evaluating the dendroclimatic potential of blue intensity on multiple conifer species from Tasmania and New Zealand. *Biogeosciences* 18:6393–6421. <https://doi.org/10.5194/bg-18-6393-2021>
- Yang B, Qin C, Wang J et al (2014) A 3,500-year tree-ring record of annual precipitation on the northeastern Tibetan Plateau. *Proc Natl Acad Sci* 111:2903–2908. <https://doi.org/10.1073/pnas.1319238111>
- Zang C, Biondi F (2015) Treeclim: an R package for the numerical calibration of proxy-climate relationships. *Ecography (cop)* 38:431–436. <https://doi.org/10.1111/ecog.01335>

**Publisher's Note** Springer Nature remains neutral with regard to jurisdictional claims in published maps and institutional affiliations.